Repair of G-quadruplex DNA Facilitated by the FANCJ Helicase and the REV1 Polymerase

Submitted by
Mena Jirjees

Biochemistry

To
The Honors College
Oakland University

In partial fulfillment of the
Requirement to graduate from
The Honors College

Mentor: Dr. Colin G. Wu
Department of Chemistry
Oakland University

April 4th, 2019

Abstract:

G-quadruplexes (G4s) are DNA structures formed by guanine-rich nucleic acids. Damaged G4s can interfere with essential cellular processes. The FANCJ helicase facilitates DNA replication through G4-forming regions. In a previous study, an "AKKQ" amino acid motif was identified within FANCJ helicase that targets G4 structures. In this project the primary aim is to test a model in which FANCJ recruits the REV1 repair protein to rescue a G4 DNA site. The approach is to first purchase FANCJ peptides and G4 DNA oligos, purify REV1 CTD and hPCNA, and then use binding experiments to measure their association reactions with each other as well as with various DNA types. The binding results thus far show that FANCJ targets a stalled replication fork at a G4-containing DNA site, and then recruits REV1 to efficiently replicate DNA across from a G-quadruplex. In the future, the plan is to reconstitute these reactions in human cells to further assess the validity of this model.

Introduction:

Guanine rich sequences can form G4s in nucleic acids. These G4-containing DNA regions are highly abundant across the human genome and are especially prone to environmental stress and oxidative damage [1-3]. G4s are formed through the folding of single-stranded DNA sequences containing four stretches of three or more successive guanines; this type of interaction is stabilized by Hoogsteen hydrogen bonding (a variation of base-pairing in nucleic acid) between guanines from each run and mono-valent cations such as potassium and sodium [4]. In Figure 1, the structure of a G-quadruplex is depicted, which shows how the four hydrogen-bonded guanines are formed from different G-tracts.

Figure 1. The structure of G-quadruplexes. (Julian Huppert, 2005)

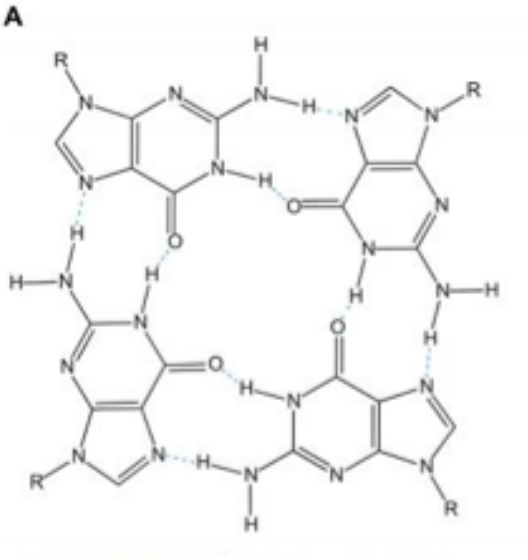

G-quadruplexes structures form inside human cells during DNA unwinding when a single-stranded DNA is exposed. If the strand is guanine rich, it can fold and form a G4 with as many as 700,000 potential G4s sequences identified within the human genome [5]. If G4s structures persist without being unfolded when the single stranded DNA is needed, they can serve as a roadblock to DNA replication fork progression by stalling respective polymerases [6-8]. Therefore, for DNA metabolism to continue undisturbed, DNA repair is necessary to unfold G-quadruplexes [8,9].

Helicases are a class of enzymes that use adenosine triphosphate (ATP) hydrolysis to fuel the process of remodeling nucleic acids and protein complexes [10,11]. FANCJ (Fanconi Anemia Complementation group J), is a human DNA helicase that repairs G4s in human cells and participates in different repair pathway including interstrand DNA crosslink (ICL) repair and homologous recombination (HR) [12-15].

Originally, FANCJ was discovered due to its binding ability with the BRCA1 tumor suppressor protein. It was later understood that FANCJ has a major role in repairing ICLs in the Fanconi Anemia pathway [16-17]. Mutations in the Fanconi anemia proteins can lead to the

disease Fanconi Anemia (FA), which includes point mutations in FANCJ helicase such as M299I, A349P, and Q944E (see Figure 2). FA is genetically inherited condition in which the bone marrow produces abnormal blood cells and prevents bone marrow from producing new normal blood cells, thereby increasing susceptibility to cancer [17,18].

Furthermore, FANCJ belongs to the Superfamily-2 (SF2) and XPD-like helicases. It has 5′→3′ directionality (the five prime to three prime directionality means that the helicase moves in that direction) [6,19]. FANCJ possesses the following domains: (HD1 and HD2) that form the motor core, an iron -sulfur cluster (FeS), and an ARCH domain inserted in the motor core of HD1 [20-22]. In addition, the FANCJ helicase binds to the C-terminal BRCT domain of BRCA1 tumor suppressor protein upon phosphorylation on serine 990 [23-24]. FANCJ has an additional unique insertion in HD1 that contains a nuclear localization sequence (NLS) and a binding site (KK141/142) for MLH1 mismatch repair protein [25,26]. Moreover, there is evidence that the Q motif in FANCJ regulates its dimerization, DNA binding, and DNA repair function. Therefore, the point mutation Q25A (Figure 2) in FANCJ impairs DNA binding and ATPase activity [13].

Figure 2 below represents the linear map of the FANCJ helicase and includes all the domains, structures, and mutations described above.

Figure 2. The linear map of the FANCJ helicase with its distinctive domains

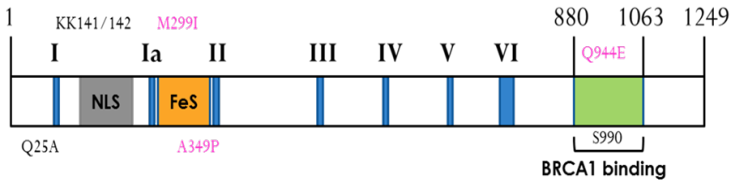

The FANCJ helicase is unique because it has the ability to participate in the repair of G4s by unfolding and refolding them. In a previous study conducted by Dr. Colin Wu and Dr. Maria Spies, an "AKKQ" amino acid motif within FANCJ was identified that allows this helicase to bind to G4 structures. Through this interaction, FANCJ is able to recognize G4-containing DNA and uses its helicase and G4-binding activities to unfold and refold these regions in repeated cycles. From this study, it has been speculated that FANCJ remains at the G4 sites and repeatedly unfolds these regions until it can hand off those structures to a polymerase that can synthesize across from the gaps. The REV1 polymerase is thought to be a good candidate for this DNA polymerase activity because it has the tendency to incorporate cytosines across from guanines [27-28,30].

The REV1 linear map includes a polymerase region (POL) involved in TLS, a CTD that is known to bypass DNA lesions that could otherwise stall polymerases, and a BRCT domain that assists with protein-protein interactions [29-31]. Figure 3 below is the linear map of the REV1 polymerase, which includes the regions discussed. Moreover, REV1 includes a PAD region that helps direct the recruitment of TLS proteins such as REV7 [32], and an ubiquitin-binding motif (UBM) that binds to ubiquitin modified PCNA [33].

Figure 3. The linear map of the REV1 polymerase with its described domains

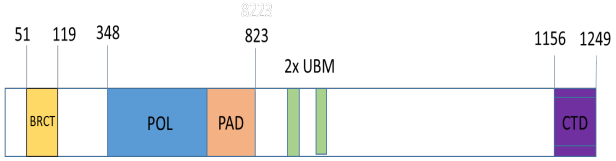

FANCJ contains residues 1001–1017 (SWSSFNSLGQYFTGKIP) that are thought to form a PCNA Interacting Peptide (PIP). The PIP is speculated to serve as a REV1 Interacting

Region (RIR) that can bind to the C-terminal domain of REV1 due to the consensus aromatic amino acids (underlined above) that have been identified in other PIPs [34]. The first reason why the REV1 polymerase is hypothesized to assist with translesion synthesis of G4s is because it has a high tendency to incorporate cytosines across from guanines [28,30]. The second reason is that cells that lack the REV1 protein tend to fail to replicate G4 forming sequences [29,30]. The main goal of this thesis is to measure the affinity between the FANCJ PIP motif and REV1 polymerase and determine if a mediator protein such as hPCNA mediates that interaction. The FANCJ helicase is thought to have a PIP motif that allows it to bind to the hPCNA protein directly and then recruit REV1 to the site by the mediator protein [34,35]. To test this hypothesis, binding assays such as BLI (Biolayer Inferometry) will be used to test which interaction has a higher affinity. Figure 4 below depicts the hypothesis in a cartoon form, which shows both the direct and indirect interaction.

Figure 4. The cartoon representation of the current hypothesis for FANCJ binding to REV1

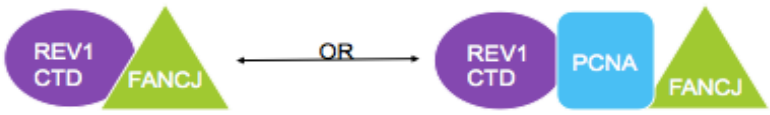

Figure 5 below represents the current model for DNA repair of the G4 complexes by FANCJ helicase. It contains G4 complex recognition sites within its helicase domain 1 (HD1), which contain the following amino acid sequence (129- PEKTTLAAKLSAKKQ-143). In particular, the "AKKQ" motif in FANCJ allows the helicase to bind to G4 complexes [27,36].

When G4 complexes form in guanine-rich single stranded DNA, the FANCJ "AKKQ" motif is recruited to the G4 site to sustain DNA replication by repeatedly folding and refolding the G4-forming sequences. In the current model proposed by Dr. Wu and Dr. Spies, the FANCJ helicase is thought to recruit a DNA synthesis polymerase such as REV1 through direct interactions with PIP-RIR sequences, or through an indirect mechanism with hPCNA mediating the interaction [27,34-35,37].

Figure 5. Current model for DNA repair of G4 complexes by the FANCJ helicase. (Colin Wu and Maria Spies, 2016)

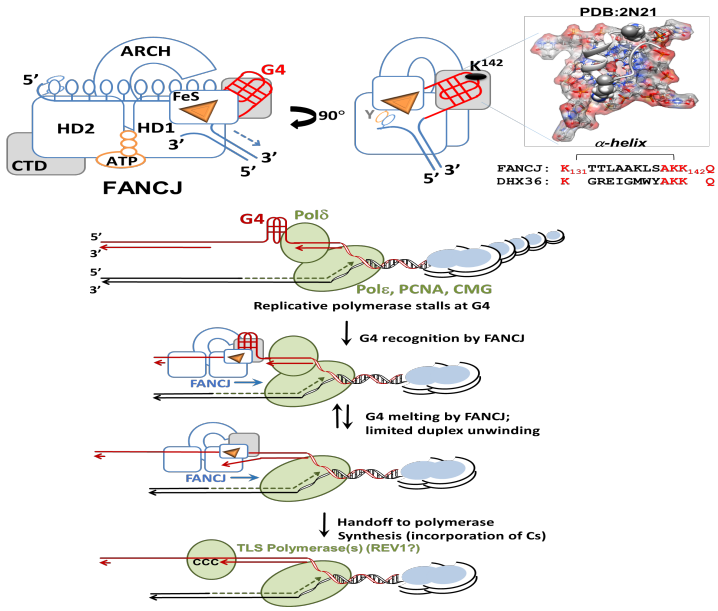

In summary, persistent G4 structures can interfere with essential cellular processes such as DNA replication and RNA transcription. A specialized protein such as FANCJ helicase is needed to unfold G-quadruplexes [5,8,32,37]. The primary focus of this project is to explore the

molecular mechanism by which damaged DNA is recognized and repaired by DNA repair enzymes.

Aims:

1. To investigate if the interaction between REV1 CTD and FANCJ helicase is mediated by hPCNA
    a. Purify recombinant REV1 CTD and hPCNA
    b. Examine the affinity between FANCJ PIP and REV1 CTD
    c. Measure the affinity between FANCJ PIP and hPCNA
2. To determine how FANCJ recognizes and repairs G-quadruplexes
    a. Examine if the "AKKQ" motif can alone recruit FANCJ to G4s

Objectives:

1. REV1 has a strong preference to incorporate cytosine across from guanine, so it has been suggested to be the repair polymerase specialized in replicating DNA across from the G-quadruplex. The next step will be testing through binding assays whether FANCJ PIP functions to recruits REV1 directly to the site, or if the FANCJ PIP binds to REV1 indirectly.
2. In a study conducted by Dr. Wu and Dr. Spies, the "AKKQ" motif within FANCJ was recognized to participate in G4 recognition. In this thesis, binding assays will be used to measure the affinity between FANCJ "AKKQ" motif and G4 DNA oligos and determine whether the motif alone can recruit FANCJ to G4s.

Methodology:

The main approach is to purify recombinant REV1 CTD and hPCNA and then use binding assays to study their interactions with the PCNA Interacting Peptide (PIP) region of FANCJ that is suspected to participate in protein-protein interactions. These results can be used to create an interaction map of the current recruitment model that describes a mechanism by which the FANCJ helicase recognizes G4s and is then thought to recruit the DNA repair polymerase REV1.

REV1 and hPCNA were produced and expressed in *E. coli.* Next, Nickel Affinity Chromatography was used to isolate REV1 and hPCNA from other endogenous bacterial proteins. The purity of the samples was assessed by gel electrophoresis. FANCJ peptide, G4 DNA, and other DNA substrates were purchased commercially from Integrated DNA Technologies. The binding interactions were monitored using BLI based binding assay.

Buffers and Reagents Used

All the experiments were done using solutions that were prepared using reagent-grade chemicals and distilled water. Additionally, the buffers and reagents were filtered using a 0.2 micron filter after preparation to ensure purity. For the purification of the REV1 CTD and the hPCNA proteins, the following buffers were used: lysis binding buffer (20 mM NaPi pH 7.5, 300 mM NaCl, 30 mM Imidazole, 1 mM DTT, 5% glycerol), wash buffer (20 mM NaPi pH 7.5, 30 mM NaCl, 30 mM Imidazole, 1 mM DTT, 5% glycerol), elution buffer (20 mM NaPi pH 7.5, 30 mM NaCl, 1 M Imidazole, 1 mM DTT, 5% glycerol). For the BLI assay, the following buffer was used: G4 Reaction Buffer (20 mM HEPES pH 7.5, 150 mM KCl, 5 mM TCEP, 5% glycerol).

Peptides and DNA Oligos Used

I. DNA oligos were also synthesized by IDT
   a. G4: $(TTAGGG)_4$
   b. T15G4: $T15(TTAGGG)_4$

II. FANCJ peptides were synthesized by Genscript
   a. AKKQ: (SPEKTTLAAKLSAKKQASIW)
   b. bioPIP: biotin-(SWSSFNSLGQYFTGKIP)

REV1 CTD and hPCNA Expression and Purification

I. ***Expression.*** REV1 CTD and hPCNA were expressed in *E. coli*. The plasmid for REV1 CTD was harbored by the NiCo21 strain, while the plasmid for hPCNA was harbored by the BL21 (DE3) strain. The strains were individually cultured in LB media supplemented with 50 ug/mL kanamycin. Cells were first grown in an overnight LB culture for 12 hours at 37°C after which the REV1 CTD cells were diluted 1:50 into 4 L of TB media, while the hPCNA cells were diluted 1:50 into 4 L of LB media. The resulting subcultured cells were grown until they reached an optical density (OD600) of 0.4 after which protein expression was induced by adding 1 mM IPTG (a biological reagent that help in protein expression) to each culture. After 4 hours, the 4 L of each cell type were harvested from the media culture by centrifugation for 20 minutes at 4,000 RPM and 4°C. The cell pellets were then stored at -80°C until lysis by freeze thaw for purification.

II. ***Purification.*** The REV1 CTD and hPCNA cell pellets were resuspended in lysis binding buffer and 1 mM PMSF, and the lysates were then sonicated for 15 min at

45% amplitude, which were used to break open the cells. The lysed cells were then centrifuged for 1.5 hours (18,000 RPM, 4°C) to obtain the soluble REV1 CTD and hPCNA proteins, referred to as the supernatant. Next, the supernatants were filtered using 0.45 micron filter, and incubated with the agarose resins with rotation at 4°C for 1 hour. The resins were washed with lysis binding buffer and wash buffer to eliminate impurities. Finally, REV1 CTD and hPCNA proteins were eluted from the column using the elution buffer. Protein aliquots were snap frozen in liquid nitrogen and stored at -80°C until further use for the BLI assay. To assess the presence and purity of the REV1 CTD and hPCNA, the eluted proteins were prepared first by adding 4x laemmli buffer (used for denaturing) and loaded on 15% polyacrylamide gel. After gel electrophoresis was finished, the REV1 CTD and hPCNA proteins were visualized with coomassie blue staining.

DNA and Protein Binding Assays

Biolayer Interferometry examines the interference pattern of white light reflected from the immobilized surface and the internal surface. BLI uses a biosensor (an analytical device used to detect chemical substances) that is coated and bonded to biological molecules such as steptavidin. BLI works by monitoring real time interactions between two different molecules, with one being mobilized on the biosensor surface and the other kept in solution.

When a biomolecule is immobilized on the biosensor, the increase in thickness of the "biolayer" at the sensor tip alters the interference pattern. In this project, the first BLI assay goal was to measure the affinity between the FANCJ PIP motif and the REV1 CTD or the hPCNA

protein to determine if FANCJ PIP functions as a RIR to recruit REV1 polymerase to G4s. The second BLI assay goal was to test the interaction between the "AKKQ" motif and G4 DNA oligos or T15G4 DNA oligos to see if the "AKKQ" motif alone can recruit FANCJ to G4s. Figure 6 below represents a simple demonstration of how the BLI assay works. The baseline step on the graph is placing the tip of the sensor in G4 Reaction Buffer. Next, the loading step is when the biotinylated partner is captured on the sensor tip, and the tip is placed again in the G4 Reaction Buffer to wash off any excess biotinylated antigen. The association step is when the sensor tip containing the biotinylated antigen is placed in the second solution that contains the second interaction partner (ligand). Finally, the dissociation step occurs when the sensor tip is placed back once again into the G4 Reaction Buffer, where the second ligand starts to dissociate from the biotinylated molecule on the tip sensor.

Figure 6. Demonstration of the real time analysis through the BLI

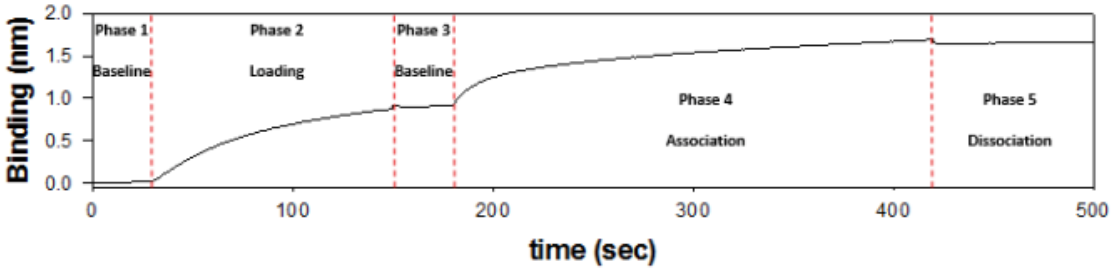

Results:

REV1 CTD and hPCNA were both produced from *E. coli* and the pure proteins were harvested and stored until purification. REV1 CTD and hPCNA were purified from other cellular proteins using gravity column chromatography and the proteins were loaded on 15% polyacrylamide gel and separated by SDS-PAGE electrophoresis. Figure 7 shows a polyacrylamide gel of the purification of the REV1 CTD and hPCNA protein. For REV1 CTD, NiCo21 cells were used. In Figure 7A, Lane 1 depicts the protein standard (a set of known protein molecular weights) that is used to compare the mobility of the known proteins' molecular weights to the protein-of-interest band. Lane 4 identifies the purified REV1 CTD running at approximately 12.5 kDa. For the hPCNA protein, BL21 (DE3) cells were used. In Figure 7B, Lane 1 shows the protein standard curve, while Lane 6 shows the purified hPCNA protein at approximately 36 kDa. Based on the amino acid sequence of the proteins' constructs, the predicted size of REV1 CTD is 14.5 kDa, and that for hPCNA is 29.5 kDa. The actual sizes of the proteins based on their amino acid sequences and their approximated sizes from the gels are reasonably close to each other with some small experimental error.

After purifying REV1 CTD, BLI was used to examine the interaction between FANCJ bioPIP and REV1 CTD. FANCJ bioPIP was placed on a streptavidin-coated biosensor and REV1 CTD was the mobile ligand in the test tube. The affinity and kinetics of the FANCJ bioPIP and REV1 CTD were then analyzed in real time using BLI.

Figure 8 below shows the interaction between two substrates, FANCJ bioPIP and REV1 CTD polymerase. The data for their interaction was obtained using BLI. The X-axis represents time in seconds, and the Y-axis represents the shift in optical interference. In this assay, it is assumed that the change in optical interference reports the extent of binding. The black curve

represents the raw experimental data, while the red curve is the fit to a one-to-one data model in which one molecule of REV1 CTD interacts with one molecule of FANCJ bioPIP in a single-step reaction. As observed from Figure 8, the concentration of the REV1 CTD polymerase varies from 0.125 μM to 2.0 μM, and as the concentration of the REV1 CTD polymerase substrate decreases, the binding signal decreases between the two substrates. The binding affinity between the two substrates was reported using the dissociation constant KD ($5.85 \pm 4.88\ X\ 10^{-7}\ M$), given by BLI.

The red curve in Figure 8 deviated significantly from the raw data, which indicates that the one-to-one data model is not sufficient in explaining all the binding time courses. Therefore, end point analysis was used to examine the interaction between FANCJ bioPIP and REVI CTD. In end point analysis, a point is chosen at equilibrium during the association phase in BLI. The graph in Figure 9 looks at the change in the equilibrium final point as a function of concentration. Eight total trials were conducted to examine the interaction between the two substrates. The averages of all the trials and their respective standard deviations were calculated and plotted in Figure 9. The X-axis represents the varying concentrations of the REV1 CTD polymerase from 0.125 μM to 2.0 μM, while the Y-axis represents the end point (a point chosen at 410 seconds from Figure 8). As indicated from the graph in Figure 9, the data is expected to follow a hyperbolic relationship that can be fit to a hyperbolic binding curve that the Wu laboratory is currently testing.

One of the major aims in this thesis is to test the type of interaction between FANCJ bioPIP and REV1 CTD. To achieve this goal, a mediator protein known as hPCNA was introduced to see if the interaction is direct or indirect. Two separate experiments were conducted to test the interactions. The first experiment using BLI was conducted between

FANCJ bioPIP and REV1 CTD to form the CTD-PIP interaction, while the second experiment was between FANCJ biPIP and hPCNA to form PCNA-PIP.

The plot in Figure 10 shows the interaction between the substrates, FANCJ bioPIP and REV1 CTD or hPCNA. The X-axis represents time in seconds, and the Y-axis represents the optical interference. As observed from the plot, the concentration of the REV1 CTD is 0.5 μM, the concentration of hPCNA is 1.0 μM, and FANCJ bioPIP binds with a higher affinity to REV1 CTD than to hPCNA. The dissociation constant KD for CTD-PIP ($5.85 \pm 4.88\ X\ 10^{-7}\ M$) was lower than the KD for PCNA-PIP ($2.32 \pm 2.82\ X\ 10^{-6}\ M$), which shows that FANCJ bioPIP has a higher affinity to REV1 CTD.

The next major aim in this thesis is to examine if the "AKKQ" motif alone can recruit FANCJ to G4s. BioT15G4 was placed on a streptavidin-coated biosensor, and FANCJ "AKKQ" peptide was the mobile ligand added to the solution. To explore this relationship, BLI was used to examine the affinity between the two substrates as noted in Figure 11. The X-axis represents time in seconds, and the Y-axis represents the optical interference. Again, the black curve represents the experimental data, while the red curve is the fit to a one-to-one data model in which one molecule of the "AKKQ" motif interacts with one molecule of the bioT15G4 DNA substrate. As observed from the plot, the concentration of the "AKKQ" motif in FANCJ varies from 0.46 μM to 7.5 μM and as the concentration of the "AKKQ" motif substrate decreases, the affinity also decreases between the two substrates. The binding affinity between the two substrates was reported using the dissociation constant KD ($2.61 \pm 1.36\ X\ 10^{-7}\ M$) given by BLI.

As shown from the graph in Figure 11, the raw experimental data varied from the one-to-one data model; therefore end point analysis was again used to examine the interaction between the "AKKQ" motif in FANCJ and the bioT15G4 DNA substrate. The graph in Figure 12

demonstrates this interaction using six total trials. The averages of all the trials and their respective standard deviations were calculated and plotted in Figure 12. The X-axis represents the varying concentrations of the "AKKQ" motif from 0.46 μM to 7.5 μM, while the Y-axis represents the end point (a point chosen at 440 seconds from Figure 11). As indicated from the graph in Figure 12, the relationship between the concentrations of the "AKKQ" motif and the end points is expected to fit a hyperbolic binding curve currently being tested in Dr. Wu's lab.

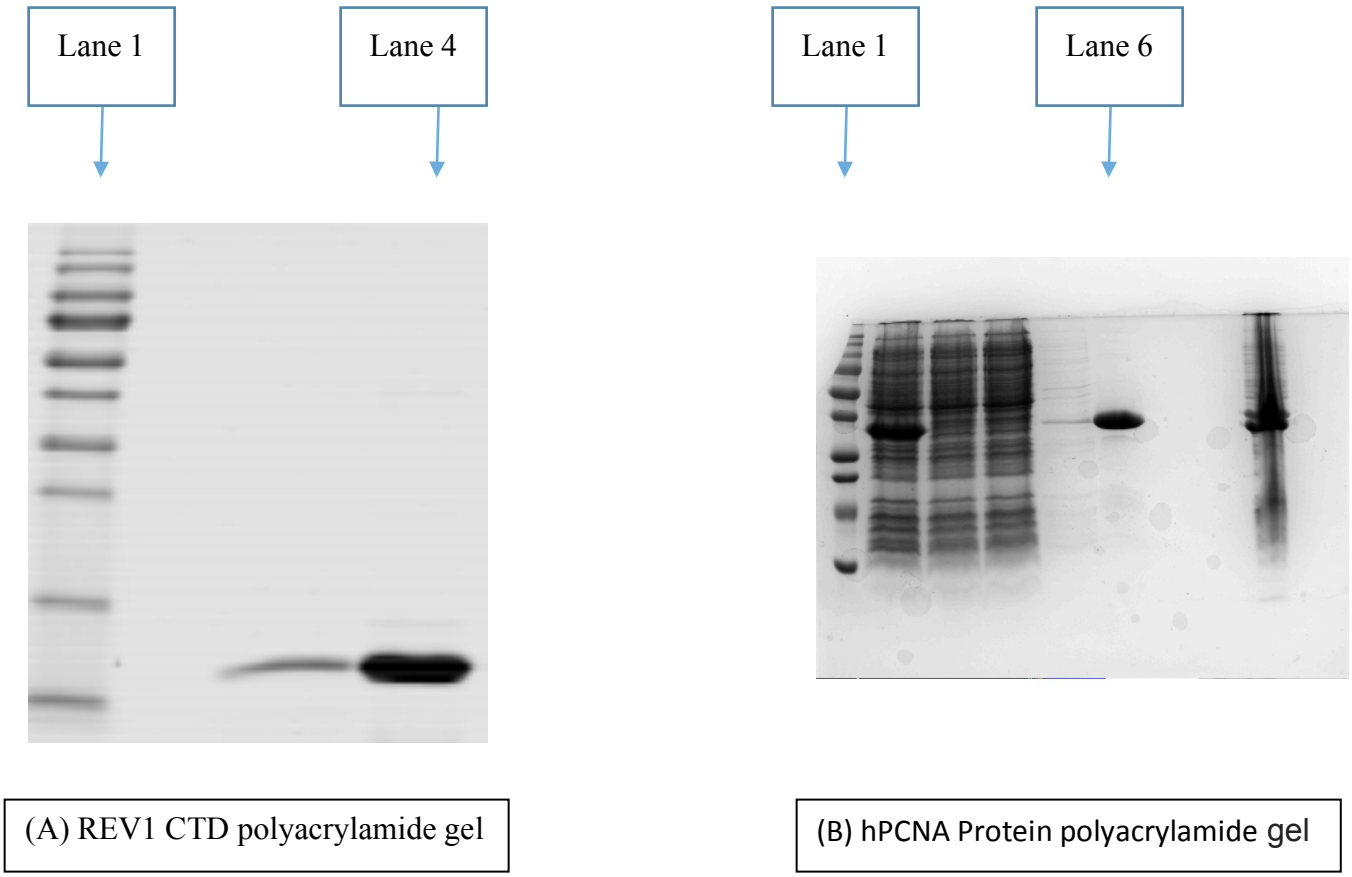

Figure 7. Coomasie blue staining of purified REV1 CTD (12.5kDa) and hPCNA protein (36kDa). Gravity chromatography was performed on the REV1 CTD using NiCo21 cells. Lane 1 shows a protein ladder (a set of known protein molecular weights used to identify the approximate size of the interest protein) while lane 4 shows the purified REV1 CTD at approximately 12.5 kDa. (B) A gravity chromatography was performed on hPCNA using BL21 (DE3) cells. Lane 1 shows a protein standard curve (a set of known protein molecular weights used to identify the approximate size of the interest protein), while lane 6 shows the purified hPCNA protein at approximately 36 kDa.

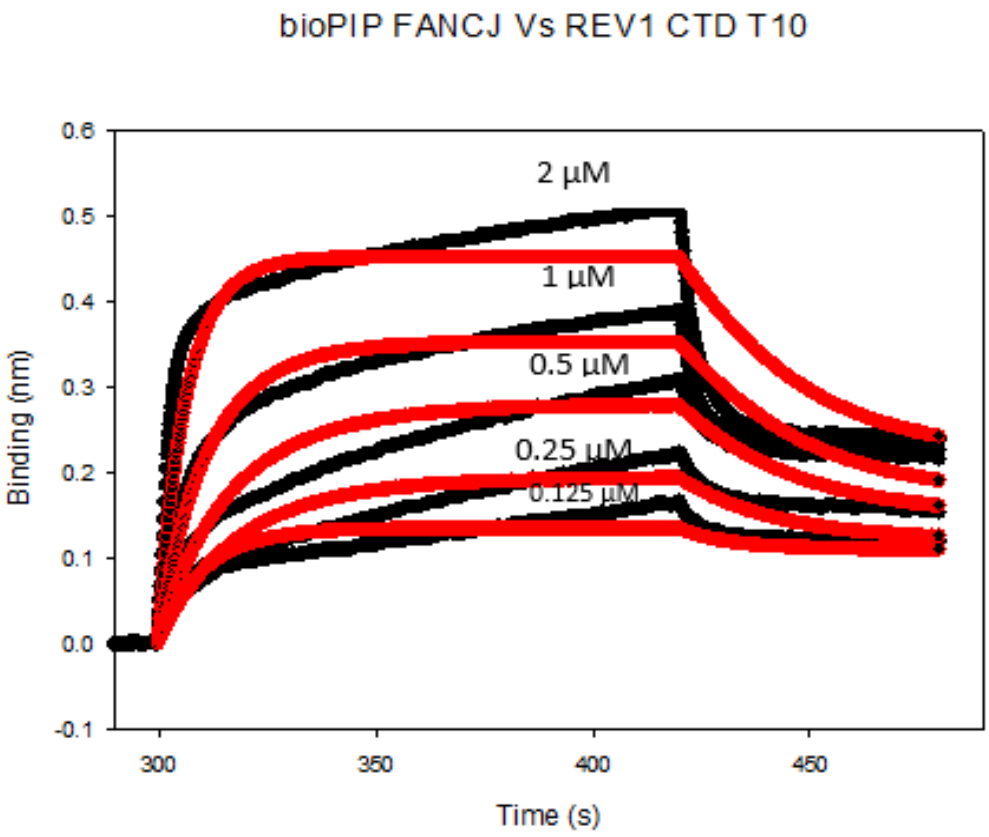

Figure 8. The Real time analysis of the binding of FANCJ PIP motif with varying REV1 CTD concentrations using BLI assay. FANCJ bioPIP was placed on a streptavidin-coated biosensor, and REV1 CTD was used as the mobile ligand in the solution. The X-axis represents time in seconds, and the Y-axis represents the shift in optical interference. The black curve represents the raw experimental data and the red curve in plot 8 is the fit to a one-to-one data model. The binding affinity between the two substrates was reported using the dissociation constant KD ($5.85 \pm 4.88\ X\ 10^{-7}\ M$) produced by BLI.

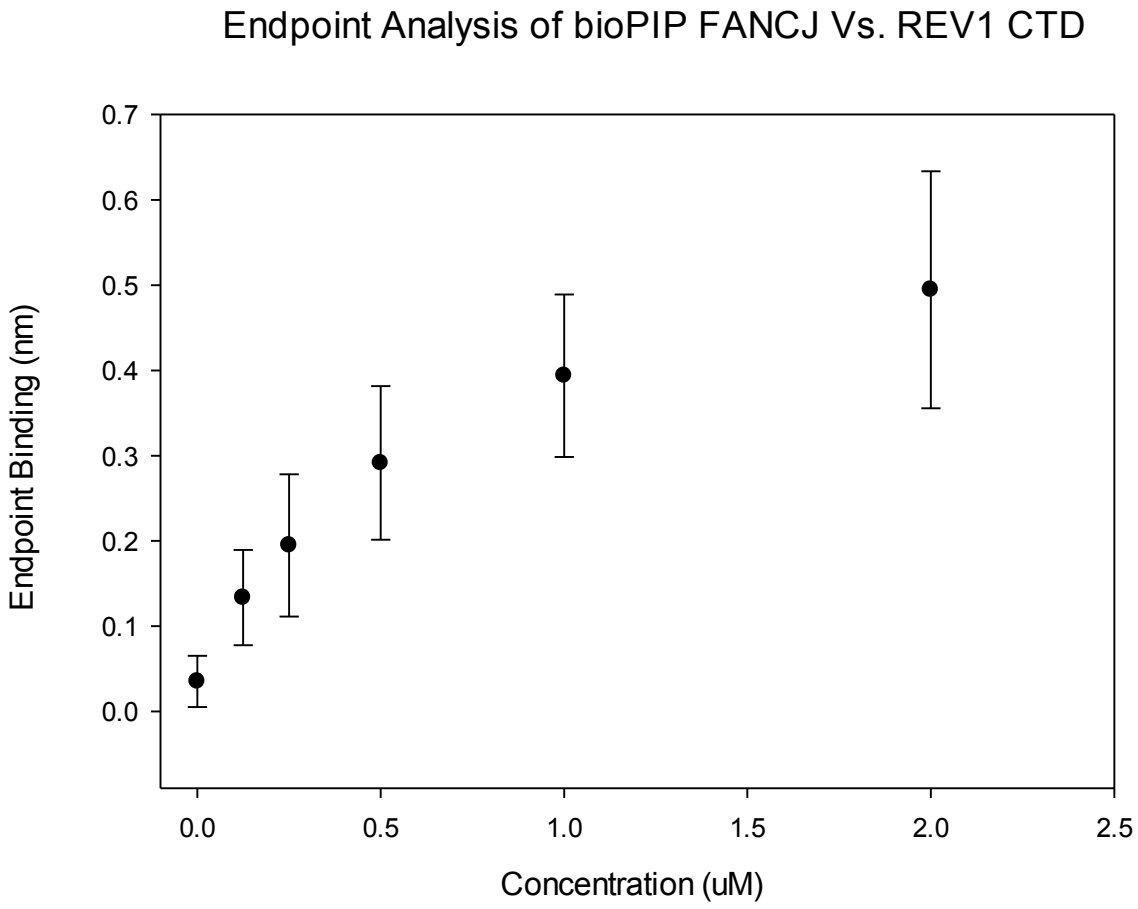

Figure 9. The end point analysis at point 410 seconds of the binding of FANCJ PIP motif with varying REV1 CTD concentrations using BLI. The REV1 CTD was purified from *E. coli* using gravity column chromatography and FANCJ peptide was purchased from Genscript. The X-axis represents concentration (μM), Y-axis represents the endpoint binding, and the error bars represent the standard deviation from 8 trials.

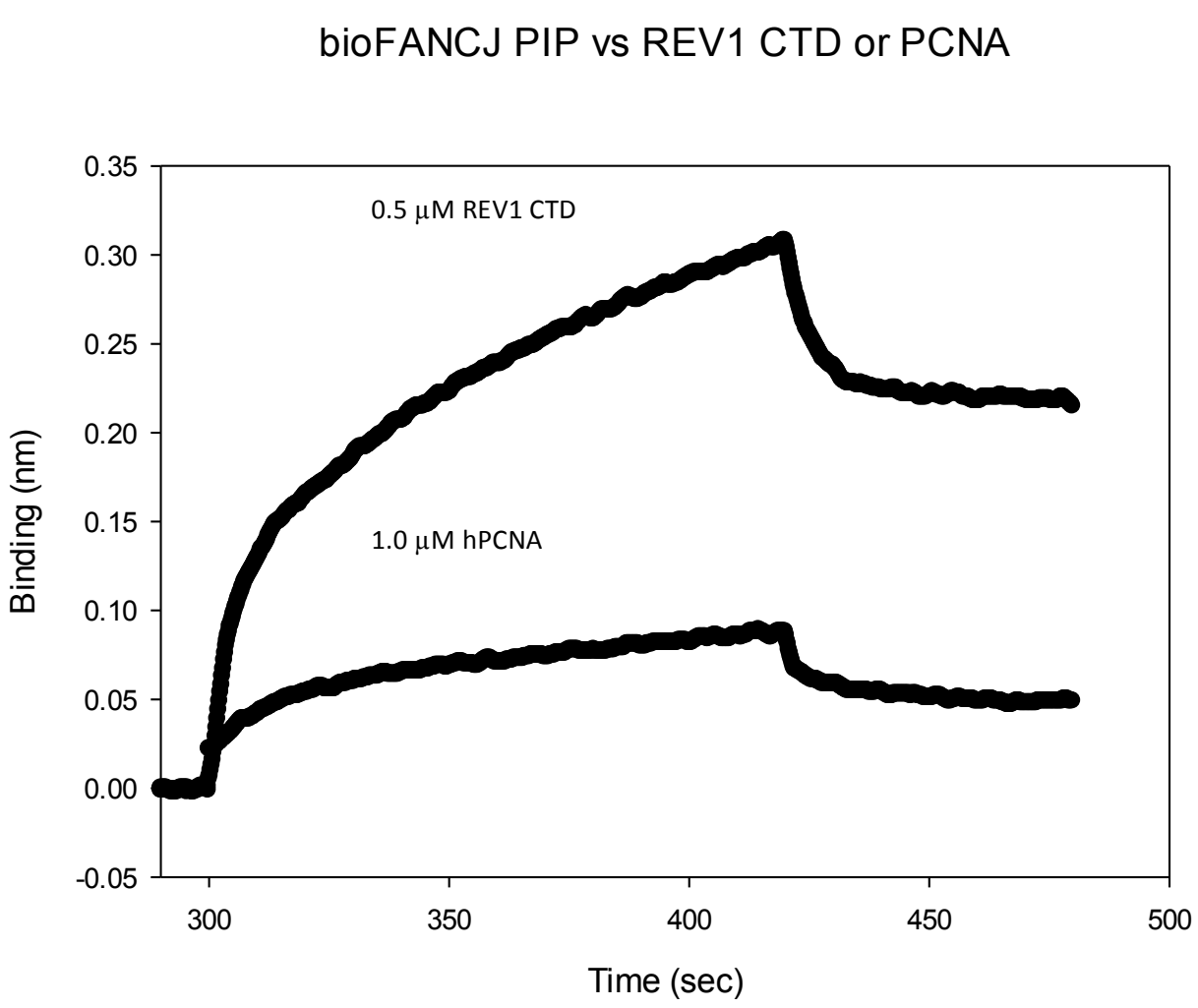

Figure 10. The binding of FANCJ PIP motif with 0.5 µM of REV1 CTD or 1.0 µM of hPCNA protein using BLI assay. The X-axis represents the time in seconds, and the Y-axis represents the affinity between the two substrates. The dissociation constant KD for CTD-PIP ($5.85 \pm 4.88\ X\ 10^{-7}\ M$) was lower than the KD for PCNA-PIP ($2.32 \pm 2.82\ X\ 10^{-6}\ M$).

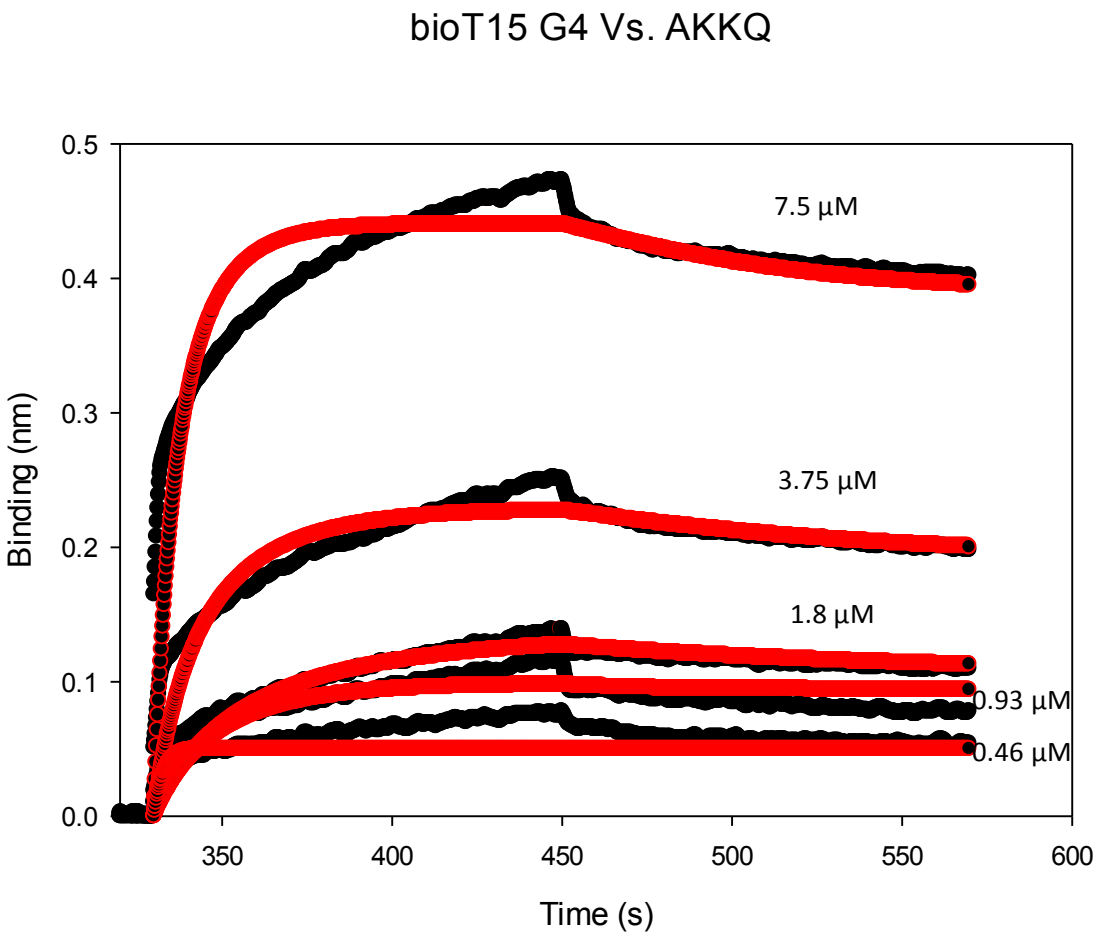

Figure 11. The binding of varying concentrations of the "AKKQ" amino acid motif within the FANCJ Helicase with a G4 DNA substrate containing 5'-dT_{15} tail. BioT15G4 was placed on a streptavidin-coated biosensor, and FANCJ "AKKQ" peptide was the mobile molecule .The X-axis represents time in seconds, and the Y-axis represents the optical interference. The red curve in plot 10 is the fit to one-to-one data model and the black curve represents the raw experimental data. The binding affinity between the two substrates was reported using the dissociation constant KD ($2.61 \pm 1.36\ X\ 10^{-7}\ M$) given by BLI.

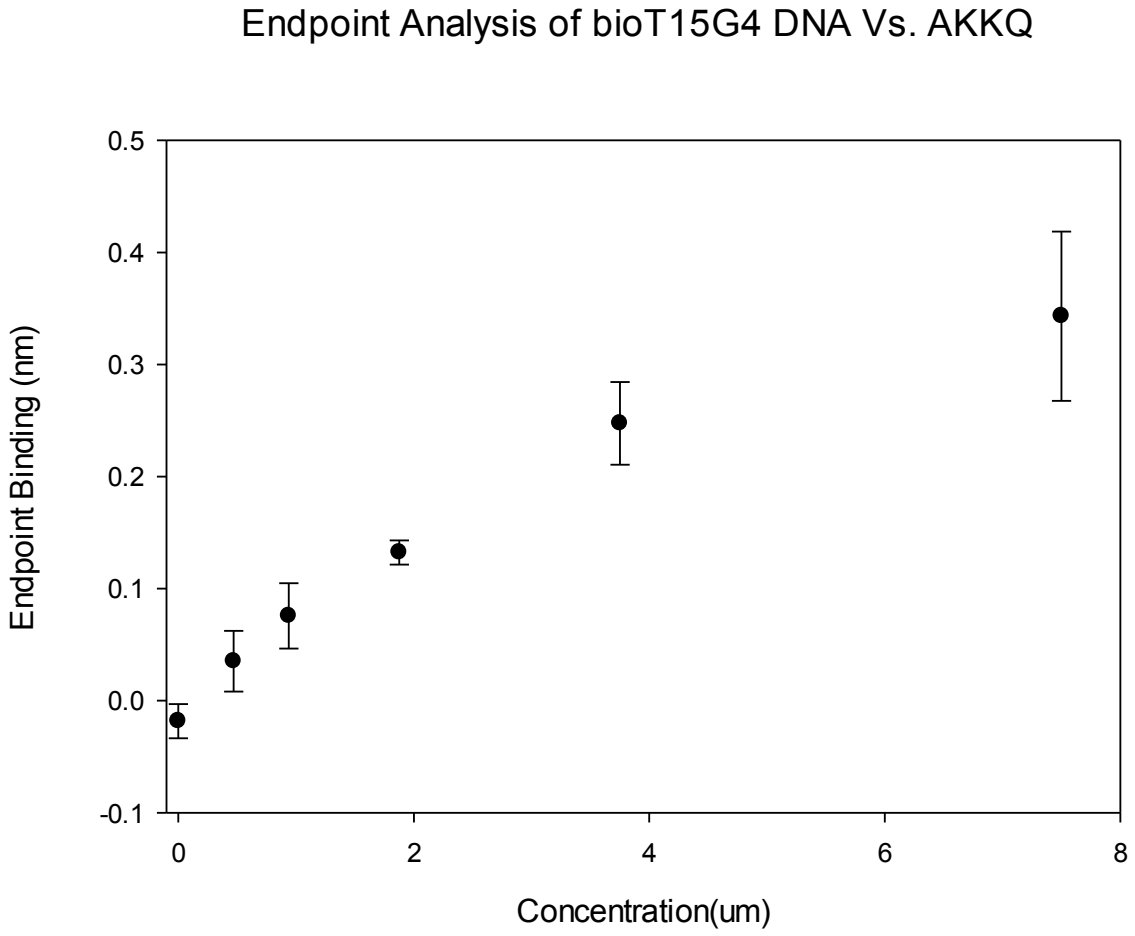

Figure 12. The end point analysis at point 440 seconds of the binding of varying concentrations of the "AKKQ" amino acid motif within the FANCJ helicase with a G4 DNA substrate containing 5'-dT_{15} tail. The X-axis represents concentration (μM), Y-axis represents the endpoint binding, and the error bars represent the standard deviation from 6 trials.

Discussion:

REV1 CTD and hPCNA protein were purified using gravity column chromatography with over 95% purity. From the polyacrylamide gels shown in Figure 7, the purified REV1 CTD ran at 12.5kDa and the hPCNA protein at 36kDa, and based on the amino acid sequence of the proteins' constructs, the predicted size of REV1 CTD is 14.5 kDa, and that for hPCNA is 29.5 kDa. The predicted sizes of the proteins and their approximated sizes from the gels are close with some experimental errors.

The experimental data from Figure 8 do not fit to a one-to-one data model; therefore an end point analysis was used in Figure 9. The reason why the black and red curves from Figure 8 do not align is because the interaction between FANCJ bioPIP and REV1 CTD is not based on one molecule of FANCJ bioPIP interacting with one molecule of REV1 CTD. From Figure 8, the binding affinity between the two substrates was reported using the dissociation constant KD ($5.85 \pm 4.88\ X\ 10^{-7}\ M$). Therefore, the binding constant between FANCJ bioPIP and REV1 CTD is relatively strong, which suggest that the FANCJ PIP could possibly function as a RIR to recruit REV1 polymerase to G4s. Moreover, BLI was used to analyze the binding of FANCJ bioPIP with 0.5 μM of REV1 CTD or 1.0 μM of hPCNA. The dissociation constant KD for CTD-PIP ($5.85 \pm 4.88\ X\ 10^{-7}\ M$) was lower than the KD for PCNA-PIP ($2.32 \pm 2.82\ X\ 10^{-6}\ M$). These results demonstrate that a direct interaction between FANCJ PIP and REV1 CTD is more favorable than an indirect interaction. An indirect interaction between FANCJ PIP and REV1 CTD cannot be completely eliminated because the mediator protein (hPCNA) still binds to FANCJ PIP. To test the indirect interaction model further, BLI experiments can be conducted between hPCNA and FANCJ PIP or REV1 CTD, and then depending on which interaction

predominately forms (PIP-hPCNA OR CTD-hPCNA), either REV1 CTD or FANCJ PIP can be added again to form PIP-hPCNA-CTD or CTD-hPCNA-PIP.

Lastly, this thesis examined if the "AKKQ" motif alone can recruit FANCJ to G4s. Figure 11 demonstrates the BLI plot of the binding of varying concentrations of the "AKKQ" amino acid motif within the FANCJ Helicase with a DNA substrate containing a 5'-dT_{15} tail. The binding affinity between the two substrates was reported using the dissociation constant KD ($2.61 \pm 1.36\ X\ 10^{-7}\ M$), which is a strong binding affinity that demonstrates that the "AKKQ" motif alone can recruit FANCJ to G4s. Figure 12 shows similar results to Figure 9 in that the black and red curves do not exactly align. Therefore, an end point analysis was used to examine the interaction between the "AKKQ" motif in FANCJ and the T15G4 DNA substrate in Figure 12. This analysis is currently being tested in the laboratory to see if the results fit to a hyperbolic binding curve, which mean that one molecule of "AKKQ" motif binds to one molecule of T15G4 DNA substrate resulting in a single equilibrium constant.

Through working on this project and conducting experiments, it was concluded that the REV1 CTD and hPCNA were purified and ready to be used for DNA binding assays. Moreover, the binding constant for CTD-PIP was relatively stronger than hPCNA-PIP, which suggests that FANCJ PIP could function as a RIR to recruit REV1 polymerase to G4s through a direct interaction. Lastly, the binding constant of the "AKKQ" motif in FANCJ and T15G4 DNA substrate strongly suggests that the "AKKQ" motif alone can recruit FANCJ to G4s. In the future, BLI experiments will be verified using the full length FANCJ helicase and REV1 polymerase, and will determine the effect of FANCJ "AKKQ" mutations on G4 repair in human cells.

References:

1. Schaffitzel, C., et al., In vitro generated antibodies specific for telomeric guanine-quadruplex DNA react with Stylonychia lemnae macronuclei. Proc Natl Acad Sci U S A, 2001. 98(15): p. 8572-7.
2. Murat, P. and S. Balasubramanian, Existence and consequences of G-quadruplex structures in DNA. Curr Opin Genet Dev, 2014. 25: p. 22-9.
3. Panich, U., et al., Ultraviolet Radiation-Induced Skin Aging: The Role of DNA Damage and Oxidative Stress in Epidermal Stem Cell Damage Mediated Skin Aging. Stem Cells Int, 2016. 2016: p. 7370642.
4. Bochman, M.L., K. Paeschke, and V.A. Zakian, DNA secondary structures: stability and function of G-quadruplex structures. Nat Rev Genet, 2012. 13(11): p. 770-80.
5. Chambers, V.S., et al., High-throughput sequencing of DNA G-quadruplex structures in the human genome. Nat Biotechnol, 2015. 33(8): p. 877-81.
6. Castillo Bosch, P., et al., FANCJ promotes DNA synthesis through G-quadruplex structures. EMBO J, 2014. 33(21): p. 2521-33.
7. Piazza, A., et al., Genetic instability triggered by G-quadruplex interacting Phen-DC compounds in Saccharomyces cerevisiae. Nucleic Acids Res, 2010. 38(13): p. 4337-48.
8. Gray, L.T., et al., G quadruplexes are genomewide targets of transcriptional helicases XPB and XPD. Nat Chem Biol, 2014. 10(4): p. 313-8.
9. Mendoza,O., Bourdoncle,A., Boule,J.B., Brosh,R.M. Jr and Mergny,J.L. (2016) G-quadruplexes and helicases. *Nucleic Acids Res.*, **44**, 1989–2006.
10. Lohman,T.M., Tomko,E.J. and Wu,C.G. (2008) Non-hexameric DNA helicases and translocases: mechanisms and regulation. *Nat. Rev. Mol. Cell Biol.*, **9**, 391–401.
11. Wu,C.G. and Spies,M. (2013) Overview: What are helicases? *Adv. Exp. Med. Biol.*, **973**, 1–16.
12. London,T.B., Barber,L.J., Mosedale,G., Kelly,G.P., Balasubramanian,S., Hickson,I.D., Boulton,S.J. and Hiom,K. (2008) FANCJ is a structure-specific DNA helicase associated with the maintenance of genomic G/C tracts. *J. Biol. Chem.*, **283**, 36132–36139.
13. Wu,Y., Shin-ya,K. and Brosh,R.M. Jr (2008) FANCJ helicase defective in Fanconia anemia and breast cancer unwinds G-quadruplex DNA to defend genomic stability. *Mol. Cell. Biol.*, **28**, 4116–4128.
14. Hiom,K. (2010) FANCJ: solving problems in DNA replication. *DNA Repair (Amst)*, **9**, 250–256.
15. Beyer,D.C., Ghoneim,M.K. and Spies,M. (2013) Structure Mechanisms of SF2 DNA Helicases. *Adv. Exp. Med. Biol.*, 47–73.
16. Cantor, S.B., et al., BACH1, a novel helicase-like protein, interacts directly with BRCA1 and contributes to its DNA repair function. Cell, 2001. 105(1): p. 149-60.
17. Litman, R., et al., BACH1 is critical for homologous recombination and appears to be the Fanconi anemia gene product FANCJ. Cancer Cell, 2005. 8(3): p. 255-65.
18. Brosh,R.M. Jr (2013) DNA helicases involved in DNA repair and their roles in cancer. *Nat. Rev. Cancer*, **13**, 542–558.
19. White,M.F. (2009) Structure, function and evolution of the XPD family of iron-sulfur-containing 5′–>3′ DNA helicases. Biochem. Soc. Trans., 37, 547–551.

20. Wolski,S.C., Kuper,J., Hanzelmann,P., Truglio,J.J., Croteau,D.L., Van Houten,B. and Kisker,C. (2008) Crystal structure of the FeS cluster-containing nucleotide excision repair helicase XPD. *PLoS Biol.*, **6**, e149.
21. Fan,L., Fuss,J.O., Cheng,Q.J., Arvai,A.S., Hammel,M., Roberts,V.A., Cooper,P.K. and Tainer,J.A. (2008) XPD helicase structures and activities: insights into the cancer and aging phenotypes from XPD mutations. *Cell*, **133**, 789–800.
22. Liu,H., Rudolf,J., Johnson,K.A., McMahon,S.A., Oke,M., Carter,L., McRobbie,A.M., Brown,S.E., Naismith,J.H. and White,M.F. (2008) Structure of the DNA repair helicase XPD. *Cell*, **133**, 801–812.
23. Cantor,S.B., Bell,D.W., Ganesan,S., Kass,E.M., Drapkin,R., Grossman,S., Wahrer,D.C., Sgroi,D.C., Lane,W.S., Haber,D.A. *et al.* (2001) BACH1, a novel helicase-like protein, interacts directly with BRCA1 and contributes to its DNA repair function. *Cell*, **105**, 149–160.
24. Clapperton,J.A., Manke,I.A., Lowery,D.M., Ho,T., Haire,L.F., Yaffe,M.B. and Smerdon,S.J. (2004) Structure and mechanism of BRCA1 BRCT domain recognition of phosphorylated BACH1 with implications for cancer. *Nat. Struct. Mol. Biol.*, **11**, 512–518.
25. Cantor,S.B. and Xie,J. (2010) Assessing the link between BACH1/FANCJ and MLH1 in DNA crosslink repair. *Environ. Mol. Mutagen.*, **51**, 500–507.
26. Peng,M., Litman,R., Xie,J., Sharma,S., Brosh,R.M. Jr and Cantor,S.B. (2007) The FANCJ/MutLalpha interaction is required for correction of the cross-link response in FA-J cells. *EMBO J.*, **26**, 3238–3249.
27. Wu, C.G., and Spies, M. (2016) G-quadruplex recognition and remodeling by the FANCJ helicase. *Nucleic Acids Res* 44(18), 8742-8753.
28. Sarkies,P., Murat,P., Phillips,L.G., Patel,K.J., Balasubramanian,S. and Sale,J.E. (2012) FANCJ coordinates two pathways that maintain epigenetic stability at G-quadruplex DNA. *Nucleic Acids Res.*, **40**, 1485–1498.
29. Eddy, S., et al., Human Rev1 polymerase disrupts G-quadruplex DNA. Nucleic Acids Res, 2014. 42(5): p. 3272-85.
30. Sarkies, P., et al., Epigenetic instability due to defective replication of structured DNA. Mol Cell, 2010. 40(5): p.703-13.
31. Jansen JG, Tsaalbi-Shtylik A, Langerak P, Calleja F, Meijers CM, Jacobs H, et al. The BRCT domain of mammalian Rev1 is involved in regulating DNA translesion synthesis. Nucleic Acids Res. 2005; 33 (1):356–65.
32. Masuda Y, Ohmae M, Masuda K, Kamiya K (2003). "Structure and enzymatic properties of a stable complex of the human REV1 and REV7 proteins". *J. Biol. Chem*. **278** (14): 12356–60.
33. Guo C., Tang T.S., Bienko M., Parker J.L., Bielen A.B., Sonoda E., Takeda S., Ulrich H.D., Dikic I., Friedberg E.C. Ubiquitin-binding motifs in REV1 protein are required for its role in the tolerance of DNA damage. Mol. Cell. Biol. 2006; 26:8892–8900.
34. Boehm,E.M., Powers,K.T., Kondratick,C.M., Spies,M., Houtman,J.C. and Washington,M.T. (2016) The proliferating cell nuclear antigen (PCNA)-interacting protein (PIP) motif of DNA polymerase eta mediates its interaction with the C-terminal domain of Rev1. *J. Biol. Chem.*, **291**, 8735–8744.

35. Boehm, E.M. and M.T. Washington, R.I.P. to the PIP: PCNA-binding motif no longer considered specific: PIP motifs and other related sequences are not distinct entities and can bind multiple proteins involved in genome maintenance. Bioessays, 2016.
36. Heddi,B., Cheong,V.V., Martadinata,H. and Phan,A.T. (2015) Insights into G-quadruplex specific recognition by the DEAH-box helicase RHAU: Solution structure of a peptide-quadruplex complex. *Proc. Natl. Acad. Sci. U.S.A.*, **112**, 9608–9613.
37. Bharti S.K., Sommers J.A., George F., Kuper J., Hamon F., Shin-ya K., Teulade-Fichou M.P., Kisker C., Brosh R.M., Jr Specialization among iron-sulfur cluster helicases to resolve G-quadruplex DNA structures that threaten genomic stability. J. Biol. Chem. 2013;288:28217–28229.